

## Artigos

### Estimation of wood volume of *Eucalyptus dunnii* and *urograndis* of different ages using TM/Landsat 5<sup>i</sup>

Estimativa de volume de madeira de *Eucalyptus dunnii* e *urograndis* de diferentes idades utilizando TM/Landsat 5<sup>i</sup>

Laura Camila de Godoy Goergen<sup>I</sup>   
Igor da Silva Narvaes<sup>II</sup>   
Marcos Adami<sup>III</sup> 

<sup>I</sup>Secretaria Municipal do Meio Ambiente de Curitiba, Curitiba, PR, Brazil

<sup>II</sup>Instituto Nacional de Pesquisas Espaciais, Santa Maria, RS, Brazil

<sup>III</sup>Instituto Nacional de Pesquisas Espaciais, Belém, PA, Brazil

## ABSTRACT

The aim of this study was the generation of trade volume models with bark (VB) in *Eucalyptus dunnii* and *urograndis* stands at different growth site conditions, using reflectance data from different regions of the electromagnetic spectrum and vegetation indices. The multiple linear regressions generated, resulting in three predictive models, being the most significant ones, in decreasing order were for the species of *Eucalyptus dunnii* and *Eucalyptus urograndis* of 50 and 59 months of age, respectively, followed by the model for 25-month old *Eucalyptus urograndis*. Although, the regression equation for 34-month old *Eucalyptus dunnii* was not significant. The vegetation index adjusted to the soil (SAVI 0.5) was relevant in the construction of the three models due to the different degrees of contribution of the soil component, as a result of the non-closure of the crowns in young stands at different ages. The short wave-infrared region (SWIR 1 – TM5) also composed the models of *Eucalyptus dunnii* and *Eucalyptus urograndis*, analyzed together and the predictive model for *Eucalyptus dunnii*, demonstrating the importance of the forest canopy structure because this region of the electromagnetic spectrum is related to increased lignin content and because of the evolution of its productive capacity.

**Keywords:** Optical remote sensing; Spectral bands; Vegetation indices; Predictive models

## RESUMO

---

O objetivo deste estudo foi a geração de modelos de volume comercial com casca (Vcc) em povoamentos de *Eucalyptus dunnii* e *urograndis* em diferentes estágios de crescimento e condições de sítio, utilizando dados de reflectância das diferentes regiões do espectro eletromagnético e de índices de vegetação. As regressões lineares múltiplas geradas resultaram em três modelos preditivos, sendo que os mais significativos, em ordem decrescente foram para as espécies de *Eucalyptus dunnii* e *Eucalyptus urograndis* com 50 e 59 meses de idade, respectivamente, seguido pelo modelo para *Eucalyptus urograndis* de 25 meses, apesar da equação de regressão para *Eucalyptus dunnii* de 34 meses, não tenha sido significativa. O índice de vegetação ajustado ao solo (SAVI 0,5) mostrou-se relevante na construção dos três modelos, pelos diferentes graus de contribuição da componente solo, decorrente do não fechamento das copas em povoamentos jovens de diferentes idades. A região do infravermelho de ondas curtas (SWIR 1) também compôs os modelos de *Eucalyptus dunnii* e *Eucalyptus urograndis*, analisados conjuntamente e o modelo preditivo para *Eucalyptus dunnii*, demonstrando a importância da estrutura do dossel florestal por esta região do espectro eletromagnético estar relacionada ao aumento do conteúdo de lignina e em decorrência da evolução de sua capacidade produtiva.

**Palavras-chave:** Sensoriamento remoto óptico; Bandas espectrais; Índices de vegetação; Modelos preditivos

## 1 INTRODUCTION

The forest production planning is composed of several stages, among them, the forest inventory (SANQUETTA *et al.*, 2014), which main objective is the monitoring of the quantitative and qualitative characteristics of the forest. Because it is an essential activity for forest management, different ways of obtaining this information have been studied, both in conventional methods, as the demarcation of temporary and permanent plots in the field, and more recently used in a large scale, sensor technologies remote (BERRA *et al.*, 2012; GOERGEN *et al.*, 2016; ALBA *et al.*, 2017).

According to Ponzoni *et al.* (2015), one of the main expectations among users of remote sensing data is the association of the spectral characteristics of objects with their physicochemical properties, which is, in fact, the basis of the application of optical remote sensing techniques. Several studies have been carried out to estimate the biophysical variables on vegetation, through index images such as the Normalized Difference Vegetation Index (NDVI) (CANAVESI *et al.*, 2010; BERRA *et al.*, 2012), Simple Ratio Index (SR) (BERRA *et al.*, 2012), Soil-Adjusted Vegetation Index

(SAVI) (REIS *et al.*, 2018; LI *et al.*, 2019), Green NDVI (GNDVI) (KROSS *et al.*, 2015) and the Moisture Vegetation Index (MVI) (ALBA *et al.*, 2017). Studies that use these indices in a joint way with the purpose of generating predictive models of volume, biomass and consequent carbon are fundamental for the production of results compatible with those of conventional forest inventories, which will ultimately bring greater efficiency and agility and decrease of survey costs, especially in large areas to be monitored (GOERGEN *et al.*, 2016). Moreover, further studies are needed on the difference in behavior between species of the eucalyptus genus and at different stages of growth (age) and how structural and management differences will lead to spectral responses and consequently in the prediction of the productive capacity of these stands.

In this context and in view of the economic potential of eucalyptus, the aim of this study was to estimate the trade volume with bark of commercial plantations of *Eucalyptus dunnii* Maiden and *Eucalyptus urograndis* (*Eucalyptus grandis* Hill ex Maiden x *Eucalyptus urophylla* S.T. Blake), at 25, 34, 50 and 59 months of age using TM/Landsat-5 sensor images.

## 2 MATERIAL AND METHOD

The study area is located in the municipality of Alegrete, in the Campaign region of Rio Grande do Sul state (55°30'W and 29°48'S). The dominant vegetation are grasslands scattered with shrubs and trees, typical of the Pampa biome (BOLDRINI, 2009). The climate of the region, according to the classification of Köppen-Geiger, is Cfa (temperate humid with hot summers), with well-distributed rains and well-defined seasons (KUINCHTNER; BURIOL, 2001). The soil in the region classified as Argissolo Vermelho Eutrófico Arênico, according to the Brazilian System of Soil Classification (SANTOS *et al.*, 2013) and Ultisol in the Soil Taxonomy (Soil Survey Staff, 2014) with smooth undulating relief, varying from 110 to 150 m altitude.

The sampling method adopted was systematic sampling, where the sample units were obtained with intervals of 300 m between them, obeying 30 meters of border. In

this way, the sampling intensity was one sample unit per 9 ha, totaling 42 in an area of 386.6 ha planted, 23 of *Eucalyptus dunnii* Maiden and 19 of *Eucalyptus urograndis* (*Eucalyptus grandis* W. Hill ex Maiden x *Eucalyptus urophylla* S. T Blake). The forest inventory was carried out in 2009 when the crop was 34 and 25 months *Eucalyptus dunnii* and *Eucalyptus urograndis* and in 2011 already with ages of 59 and 50 months, respectively. In these plots, no silvicultural treatment, such as thinning and pruning was carried out.

All permanent forest inventory plots, located in the same field, with the same silvicultural conditions, with approximately 314 m<sup>2</sup> (10 m radius) represented the same image resolution element for each pixel of 900 m<sup>2</sup>. In the sample units, the circumference at the chest height of all individuals were measured, with the aid of the measuring tape, and the total height of 15 initial trees and five thickest trees, with the aid of a clinometer (*Haglöf Electronic Clinometer*) in the forest stand with initial plant spacing was 3.5 x 2.0 m for *Eucalyptus dunnii* and 3.5 x 2.5 m for *Eucalyptus urograndis*. The values of the plane coordinates of each sample point were gathered using Garmin Etrex Legend®.

The planting was identified from the coordinates of the central point of the plots, in the images of Landsat 5 satellite, TM sensor, orbit-point 224/81 of September 25th, 2009 and October 17th, 2011, closest to the data collection and free of clouds at the time of acquisition, considering its 16-day temporal resolution. These images were obtained free of charge from the National Institute for Space Research - INPE (2012) and were used to generate the spectral response attributes of the areas corresponding to the sampling points, after the geo-referencing and atmospheric correction operations. In the geo-referencing of the images, an orthorectified image "geocover" of the NASA page was used as the basis for the program *Global Land Cover Facility* of the University of Maryland (GUTMAN *et al.*, 2013).

For the atmospheric correction, each original image for the bands TM1 (0.45 to 0.52 µm - B: Blue), TM2 (0.52 µm to 0.60 µm - G: Green), TM3 (0.63 to 0.69 µm - R:

Red), TM4 (0.76 to 0.90  $\mu\text{m}$  - NIR: Near InfraRed), TM5 (1.55 to 1.75  $\mu\text{m}$  - SWIR1: Short Wave InfraRed 1) and TM7 (2.09 to 2.35  $\mu\text{m}$  - SWIR2: Short Wave InfraRed 2) of TM/Landsat 5, was initially converted from digital number (ND) to radiance at the top of the atmosphere (ToA using the spectral radiance parameters of the Landsat 5 satellite (CHANDER *et al.*, 2007). Then, the radiance images at the top of the atmosphere were converted to reflectance on the Earth's surface by means of the atmospheric correction algorithm called *Fast Line-of-sight Atmospheric Analysis of Spectral Hypercubes* (FLAASH), available in application *Environment for Visualizing Images* ENVI 4.5® (ITT, 2009), also used by other authors (LI *et al.*, 2020; ZHAO *et al.*, 2019; BERRA *et al.*, 2017). For each scene, information concerning the nominal altitude of the sensor, date and time of satellite pass, the center coordinates of the image, solar elevation angle, average altitude of the terrain, maximum spectral radiance values and minimum sensor and conditions atmosphere were inserted, at the time of the satellite passage (visibility, concentration of gases and aerosols). Thus, the average elevation of the terrain was assumed to be 0.14 km, the atmospheric model "*Mid-latitude summer*", the rural aerosol model with visibility adopted was 100 km.

Eleven (11) attributes of spectral responses were selected, referring to bands Landsat -5/TM (TM1, TM2, TM3, TM4, SWIR 1 -TM5 and SWIR 2 -TM7) and vegetation indices (SR, NDVI, SAVI, GNDVI and MVI; Table 1), which served as components of the explanatory variables of a multiple regression model, in order to find equations that best estimate the trade volume with bark. The reflectance values obtained using the arithmetic mean of the pixels covering the sample unit.

Initially, a descriptive analysis of the data was performed, generating a dispersion diagram between all the independent and dependent variables. The multicollinearity verification was also performed between the independent variables and the correlation between these variables and the VB (NETER *et al.*, 1996). The choice of the variables that would be, *a priori*, part of the regression model, also took into account the relationships of vegetation with each spectral range, following the literature (GOEL, 1988).

From the data adjustment, the best mathematical models were selected, based on the following statistical criteria: the coefficient of determination ( $R^2$ ), the standard error of the estimate ( $S_{yx}$ ), the value of the  $F$  statistic and the value of 95% probability of confidence (NETER *et al.*, 1996).

Table 1 – Vegetation indices used in multiple linear regression as potential explanatory variables for estimating the trade volume model with bark ( $\text{m}^3 \text{ha}^{-1}$ )

Vegetation indices	Author	Formulation
Simple Ratio (SR)	Jordan (1969)	$SR = \frac{\rho_{NIR}}{\rho_R}$
Normalized Difference Vegetation Index (NDVI)	Rouse <i>et al.</i> (1974)	$NDVI = \frac{\rho_{NIR} - \rho_R}{\rho_{NIR} + \rho_R}$
Soil-adjusted vegetation index (SAVI)	Huete (1988)	$SAVI = \frac{\rho_{NIR} - \rho_R}{\rho_{NIR} + \rho_R + L} \times (1 + L)$
Green NDVI (GNDVI)	Souza and Ponzoni (1998)	$GNDVI = \frac{\rho_{NIR} - \rho_{green}}{\rho_{NIR} + \rho_{green}}$
Moisture vegetation index (MVI)	Souza and Ponzoni (1998)	$MVI = \frac{\rho_{NIR} - \rho_{MIR}}{\rho_{NIR} + \rho_{MIR}}$

Source: Authors (2019)

In where:  $\rho_{NIR}$  = is the near infrared reflectance;  $\rho_R$  = is the reflectance in red;  $L$  = constant that minimizes the effects inherent to the soil, used in this study with a value of 0.5;  $\rho_{green}$  = is the reflectance in green;  $\rho_{MIR}$  = is the mid-infrared reflectance.

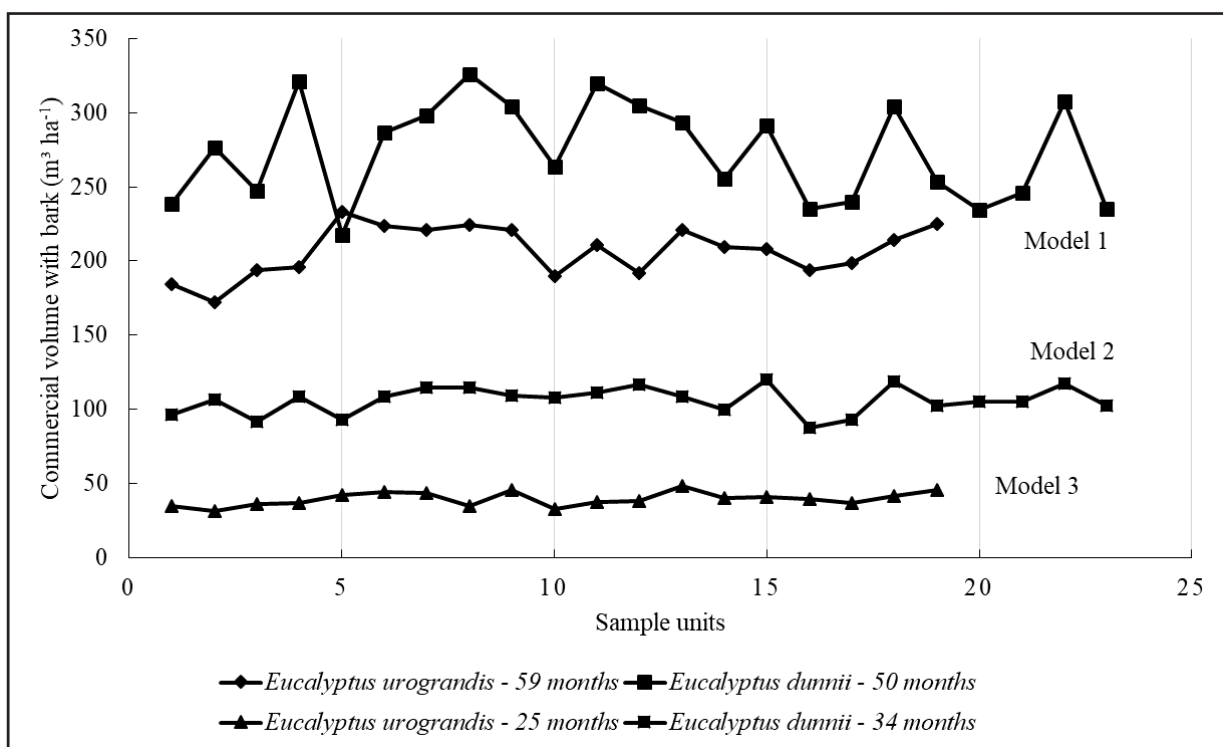
Although the sample intensity was considered sufficient for the model generation using all the observations of this forest inventory, this number was insufficient to reserve 20% of the independent observations for the validation of the model (NETER *et al.*, 1996). As a way of solving this premise, the *Bootstrap* technique was used (EFRON, 1987), which draws a number  $n$  of possible interactions for the generation of the model. In this specific case 1,000 draws were used with replacement. This method

adaptively determines the sample fraction that minimizes the asymptotic mean square error (DANIELSSON, 2001), being extended to other measures of statistical precision, such as trends and predictions of errors, and to complex data structures from a small number of samples without assumption of a specific probability density function (EFRON; TIBSHIRANI, 1997).

### 3 RESULTS AND DISCUSSION

The choice of three models was evidenced by the distinct behavior of volume with bark ( $\text{m}^3 \text{ha}^{-1}$ ) obtained from conventional forest inventory data for *Eucalyptus dunnii* and *Eucalyptus urograndis* species, aged 24 and 25 months, and by similar pattern for these two species at the age of 59 and 50 months, respectively (Figure 1).

Figure 1 – Trade volume with bark behavior ( $\text{m}^3 \text{ha}^{-1}$ ) on the sample units to *Eucalyptus urograndis* and *Eucalyptus dunnii* with differences ages (months)



Source: Authors (2019)



Because of the behavior of the trade volume with bark obtained in the forest inventory, the values of the linear coefficients of Person were generated at 95% confidence probability (Table 2). The average reflectance values found for TM3, TM4, NDVI and SR were similar to those reported by Berra *et al.* (2012) who also worked with images of the TM sensor Landsat 5, in the area of *Eucalyptus* sp. plantations, in Rio Grande do Sul state.

A significant correlation was observed between the trade volume with bark and reflectance of the spectral variables for most of the bands in the two studied ages, and for the majority of vegetation indices generated for the samples with age of 50 and 59 months for both species. The volume of wood with bark presented the highest values of significant correlation with the variables reflectance in the NIR region (TM4) and with the SAVI 0.5 vegetation index for the two ages evaluated, although the older population had a significant correlation also for the SR, MVI, NDVI indices and for the reflectance in the SWIR1 (TM5) and green (TM2) bands. Reis *et al.* (2018), evaluated the behavior of *Eucalyptus* sp. At different ages from the Landsat 5 TM spectral bands and found a significant correlation between volume and the TM4 band only in plantations with 5 years of age.

The negative correlations found between volume and TM2, TM3, TM 4 and SWIR1 -TM 5 bands are commonly reported (WATZLAWICK *et al.*, 2009; BERRA *et al.*, 2012; ALMEIDA *et al.*, 2014; REIS *et al.*, 2018; MACEDO *et al.*, 2017). However, for vegetation indices, some authors found significant positive correlations (BERRA *et al.*, 2012; ALMEIDA *et al.*, 2014; REIS *et al.*, 2018) and others, negative (WATZLAWICK *et al.*, 2009; MACEDO *et al.*, 2017), as well as in the present work, where all the significant correlations were in their totality negative ones.

According to Lu *et al.* (2004) the vegetation structure has a greater influence on the correlation between the population parameters and the reflectance values than the physiognomy or amount of biomass of each region, suggesting that, in this analysis, the age difference in the initial growth of *Eucalyptus dunnii* Maiden is preponderant in the differentiation of the canopy architecture as a relevant factor for the correlation of these explanatory variables studied.



The high correlations found for the vegetation indices are mainly due to their compositions that use essentially the spectral bands in the region of the red and infrared related electromagnetic spectrum, respectively considered as a region of strong absorption and of maximum reflectance (MACEDO *et al.*, 2017), which is why most of the vegetation indices were established.

Thus, the short wave infrared - SWIR 1 (TM5) and the SAVI 0.5 index were used for the populations of 34-month old *Eucalyptus dunnii*, although they were not significant at 0.05 ( $p$ -value = 0.1745 and 0.1677, respectively), because it showed the highest  $R^2$  and the smallest  $S_{yx}$  for both species to the 2011 inventory year and demonstrated to be a good predictor to distinguish different eucalyptus species in similar areas of the present study (GOERGEN *et al.*, 2016).

Table 2 – Pearson correlation coefficients between the trade volume of bark wood ( $m^3 ha^{-1}$ ) and the reflectance of the spectral bands and vegetation indexes for the two species and ages evaluated

Variable	VB ( <i>Eucalyptus dunnii</i> ) 34 months	VB ( <i>Eucalyptus urograndis</i> ) 25 months	VB ( <i>Eucalyptus dunnii</i> + <i>Eucalyptus urograndis</i> ) 59 e 50 months, respectively
Year	2009	2009	2011
TM1	-0.03	0.09	-0.09
TM2	0.21	0.41*	-0.54*
TM3	-0.06	0.25	-0.04
TM4	-0.32*	0.72*	-0.74*
SWIR1-TM5	-0.29	-0.39*	-0.61*
SWIR2-TM7	-0.25	0.45*	0.12
NDVI	-0.00	0.04	-0.68*
SR	0.01	-0.00	-0.70*
SAVI 0.5	-0.30	0.70*	-0.75*
MVI	0.06	0.64*	-0.66*
GNDVI	-0.27	-0.08	-0.32

Source: Authors (2019)

Note: \* Significant correlation at 5% probability, VB = volume with bark,  $m^3 ha^{-1}$ .

The same behavior was first verified for the settlement of *Eucalyptus urograndis* with 25 months, but the generated model showed that only the SAVI 0.5 variable was significant at 0.05 ( $p$ -value = 0.0008). When analyzed together, in populations of *Eucalyptus dunnii* and *Eucalyptus urograndis* at 59 and 50 months in 2011, a greater number of explanatory variables showed a significant correlation with the VB. However, only the SWIR1 (TM5) and the SAVI 0.5 index were significant at 0.05 ( $p$ -value = 0.0437 and  $1.79 \times 10^{-05}$ , respectively). The models resulting from this analysis, as well as the statistical parameters of these are presented in Table 3.

Table 3 – Regression models adjusted to estimate the volume of wood in plantations of *Eucalyptus dunnii* and *urograndis*, at different ages

Model	Dependent variable	Inventory Year	Equation	F	R <sup>2</sup>	S <sub>yx</sub> (m <sup>3</sup> ha <sup>-1</sup> )
1	VB ( <i>Eucalyptus urograndis</i> + <i>Eucalyptus dunnii</i> ) 50 e 59 months, respectively.	2011	593.80 – 376.55 (SAVI 0.5) – 2009.96 (SWIR1 – TM5) + ε	30.80*	0.61	27.58
2	VB ( <i>Eucalyptus urograndis</i> ) 25 months	2009	– 18.65 + 96.59 (SAVI 0.5) + ε	16.51*	0.49	3.42
3	VB ( <i>Eucalyptus dunnii</i> ) 34 months	2009	234.01 – 161.48 (SAVI 0.5) – 466.49 (SWIR1 – TM5) + ε	2.06	0.17	8.69

Source: Authors (2019)

In where: \* Significant at 5% probability; VB = trade volume with bark, m<sup>3</sup> ha<sup>-1</sup>; F = F value of the analysis of variance; R<sup>2</sup> = Determination coefficient; S<sub>yx</sub> = standard error of the estimate; ε = error.

For the model of *Eucalyptus urograndis* and *Eucalyptus dunnii* species, with 50 and 59 months, respectively, the variables selected were the SWIR1 band (TM5) and the soil-

adjusted vegetation index (SAVI 0.5), since they had a better response the variability of the VB, presenting the best fit to the regression line of  $R^2 = 0.61$ , in comparison to the others, besides having obtained a high correlation (78%) between the observed and estimated data. In this, the statistical parameters indicated by the standard error of the estimate ( $S_{yx}$ ) obtained a value of  $27.58 \text{ m}^3 \text{ ha}^{-1}$ , indicating 11.32% of variation in the calculation of the sample mean, due to the difference of age, site and of structural characteristics between the two species.

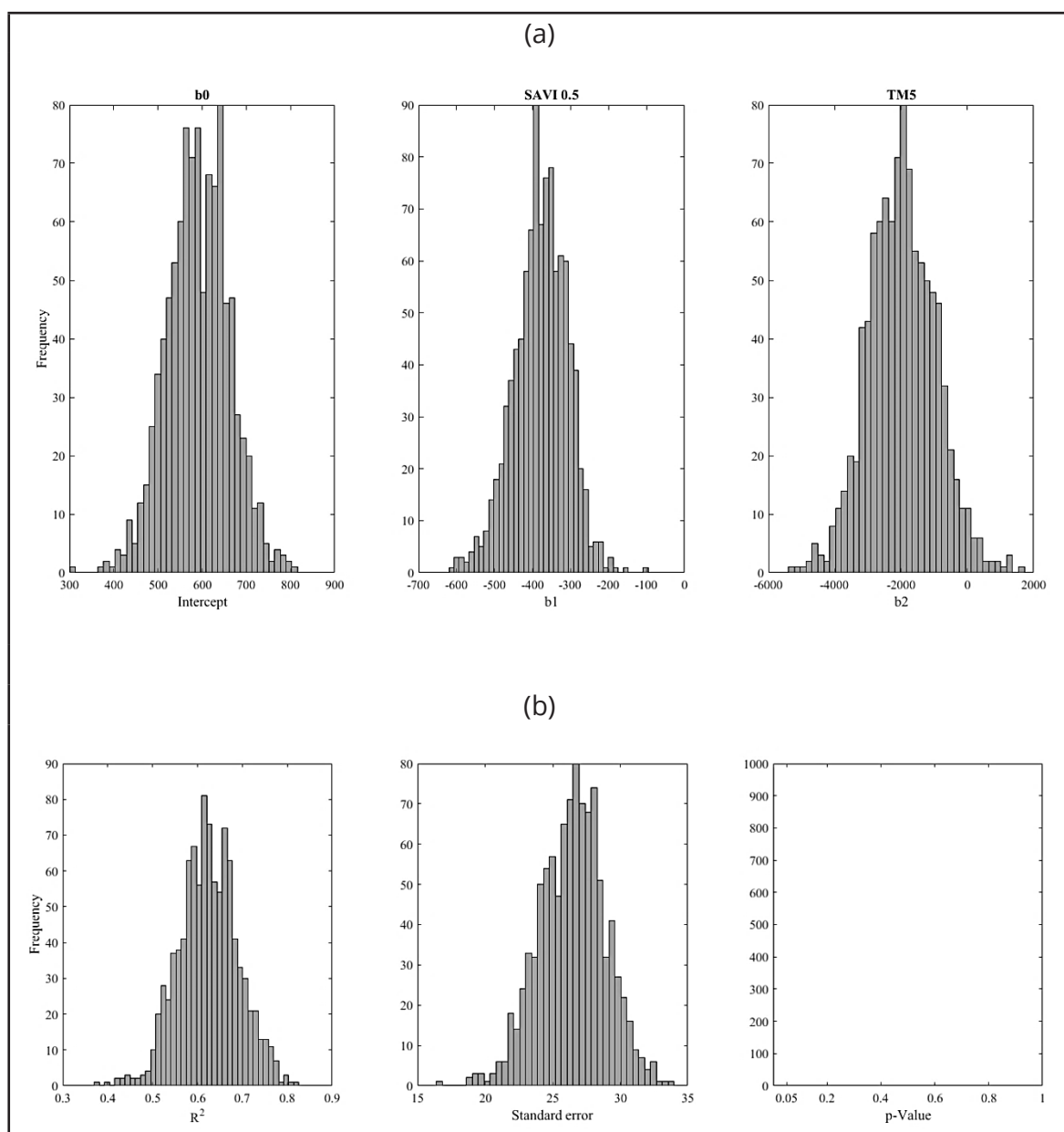
Canavesi *et al.* (2010), in the analysis of *Eucalyptus* sp. stands, through the use of hyperspectral sensors and correction of the topography effect, using data from digital terrain models from SRTM (*Shuttle Radar Topography Mission*), found consistent results in the generation of predictive volume models, with coefficient of determination reaching up to 0.70. Dube and Mutanga (2015), using images from Landsat 7/ETM+ and Landsat 8/OLI, found satisfactory adjustments for the volumetric modeling of *Eucalyptus dunnii* and *Eucalyptus grandis*, reaching  $R^2$  values of 0.66; 0.52 and absolute mean error of 9.56; 18.52, respectively, when these two sensor systems are combined.

Despite the distinct site conditions of this study to the three models generated, a similar trend was found in Alba *et al.* (2017) to *Eucalyptus grandis* populations when analyzing the ages of 4, 18 and 23 years, using OLI/Landsat-8 data, in the coastal region of the Rio Grande do Sul State.

The validation of the model, calculated by the *Bootstrap* method (Figure 2a), showed that although the model is significant, the best fit was for the independent SAVI 0.5 variable, since none of the 1000 simulations had a value equal to zero, while for the TM5 independent variable a small number of observations obtained values equal to zero, evidencing the smaller contribution of this in the composition of the final model. The significance of the model is also justified by the large distribution of

the  $R^2$  values and the estimated variance of the error being concentrated around the mean values found, in addition to all the observations from these interactions to prove their fit to the data of field ( $p$ -value  $\ll 0.05$ ; Figure 2b).

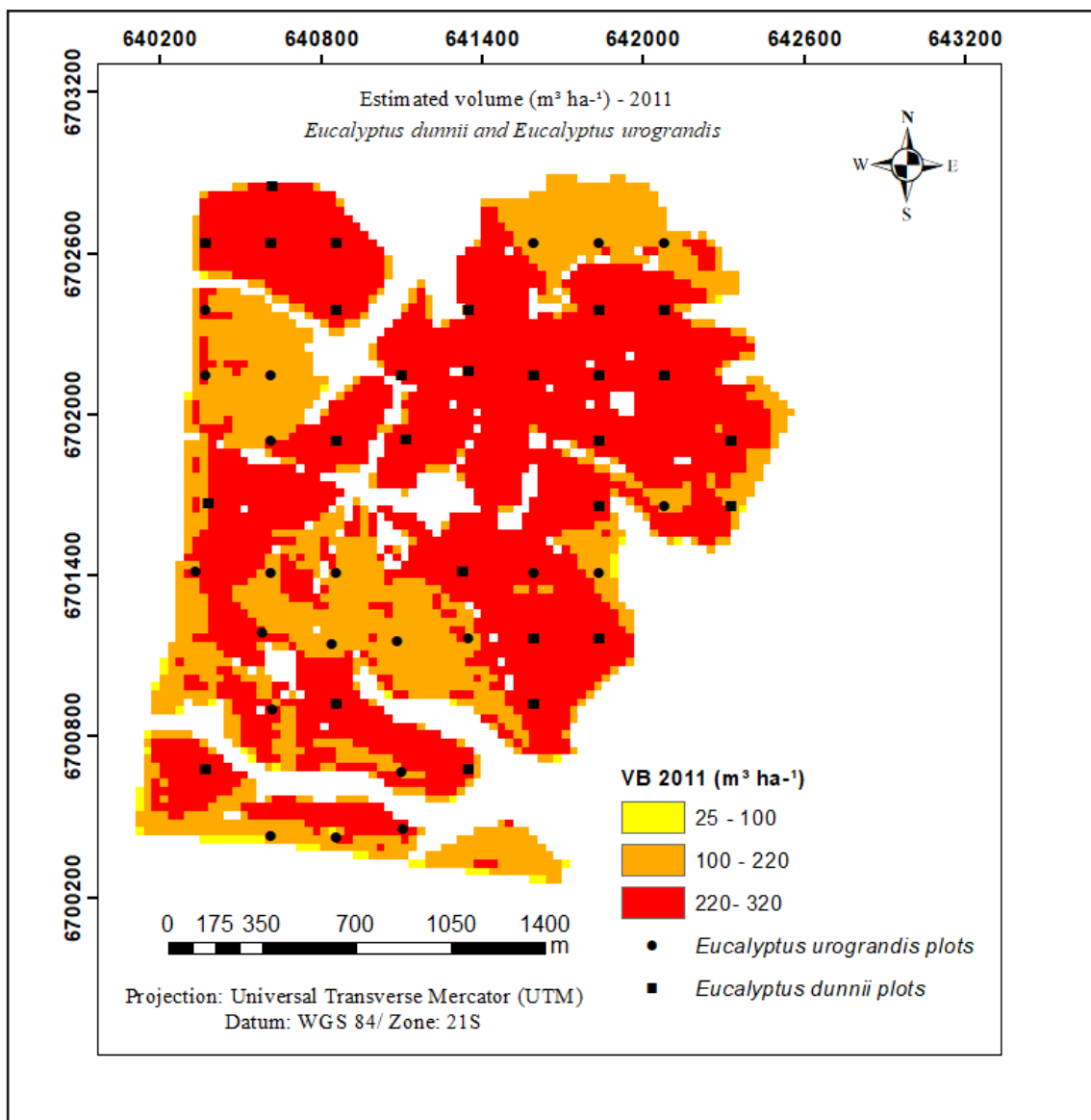
Figure 2 – Prediction model of trade volume with bark in stands of *Eucalyptus dunnii* and *Eucalyptus urograndis* of 59 and 50 months, respectively. (a) coefficients of the model and; (b) statistical criteria of coefficient of determination ( $R^2$ ), estimation of error variance and  $p$ -value, to 95% probability of confidence



Source: Authors (2019)

The efficiency of the model allowed to generate VB distribution surface ( $\text{m}^3 \text{ha}^{-1}$ ) for these stands (Figure 3), indicated higher volume values for *Eucalyptus dunnii* stands and smaller ones for *Eucalyptus urograndis*, corresponding to the regions that most of the sample units of these species are materialized.

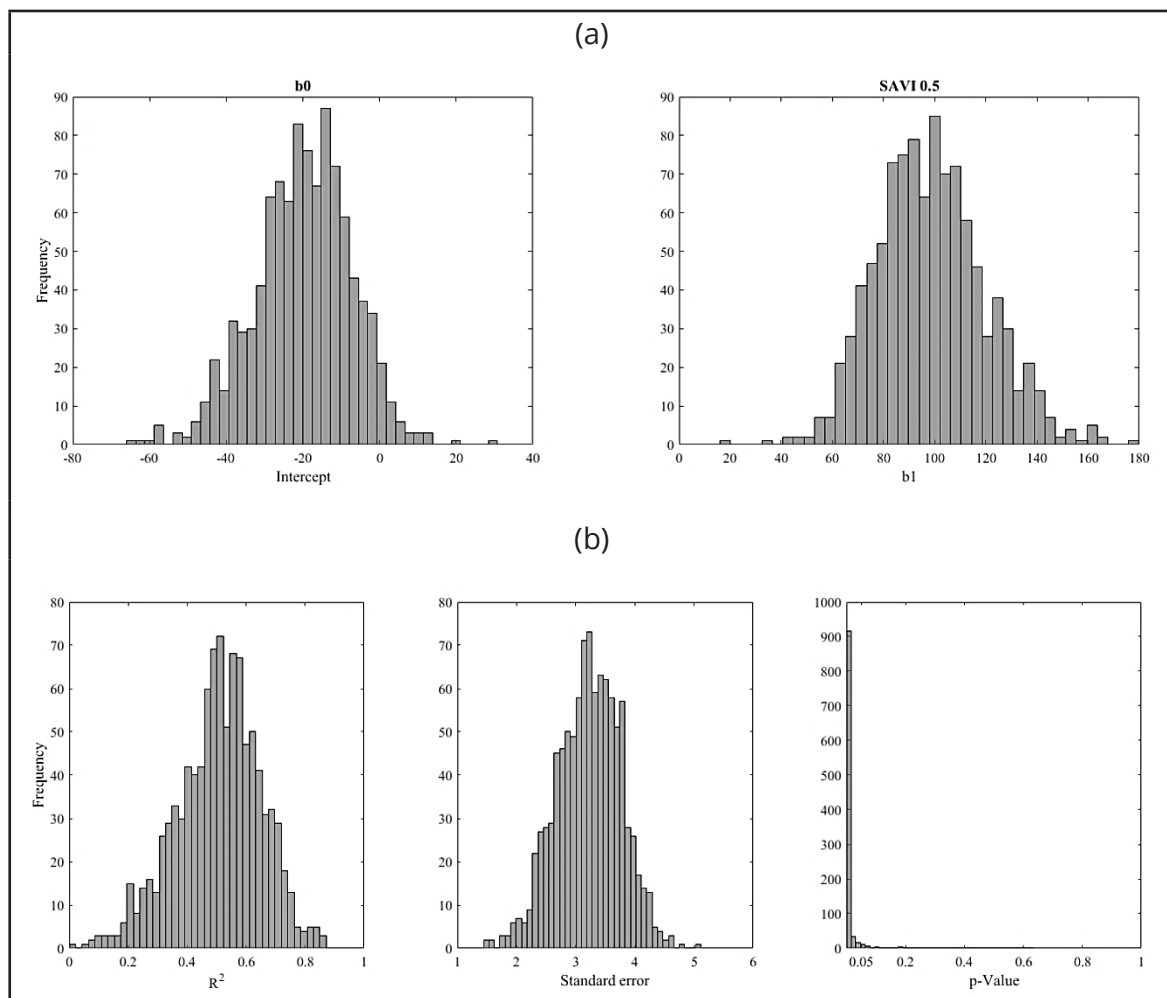
Figure 3 – Distribution map of trade volume with bark (VB -  $\text{m}^3 \text{ha}^{-1}$ ) of stands of *Eucalyptus dunnii* and *Eucalyptus urograndis* of 59 and 50 months, respectively. The squares and points refer to the spatial location of the sample units used in the forest inventory



Source: Authors (2019)

In the model generated for 25-month old stands of *Eucalyptus urograndis*, the *Soil-Adjusted Vegetation Index* (SAVI 0.5) was the one that best answered the variability of the stored VB, with a regression line adjustment of  $R^2 = 0.49$  and low mean value of the standard error of the estimate ( $S_{yx} = 3.42 \text{ m}^3 \text{ ha}^{-1}$ ), and high correlation (70%) between the observed and estimated values. The relative importance of SAVI 0.5 in the elaboration of volume prediction models, in this case, is related to greater exposure of the soil as the closure of the canopies has not yet occurred.

Figure 4 – Prediction model of trade volume with bark in 25-month old *Eucalyptus urograndis* stands. (a) coefficients of the model and; (b) statistical criteria of coefficient of determination ( $R^2$ ), estimation of error variance and p value, at 95% probability of confidence



Source: Authors (2019)

The results found in the present study, although significant were lower than those reported by Macedo *et al.* (2017), which obtained  $R^2$  of 0.70, using the SAVI index to estimate the volume of *Eucalyptus* sp. with an age of less than three years, which can be explained in part by the use of very high spatial resolution images (0.50 m) and consequently, capable of recording greater reflectance information of the soil area, increasing the relative importance of this component, compared to the Landsat-5/TM images used in this study, with a spatial resolution of 30 m where the spectral mixture between vegetation and soil is much larger.

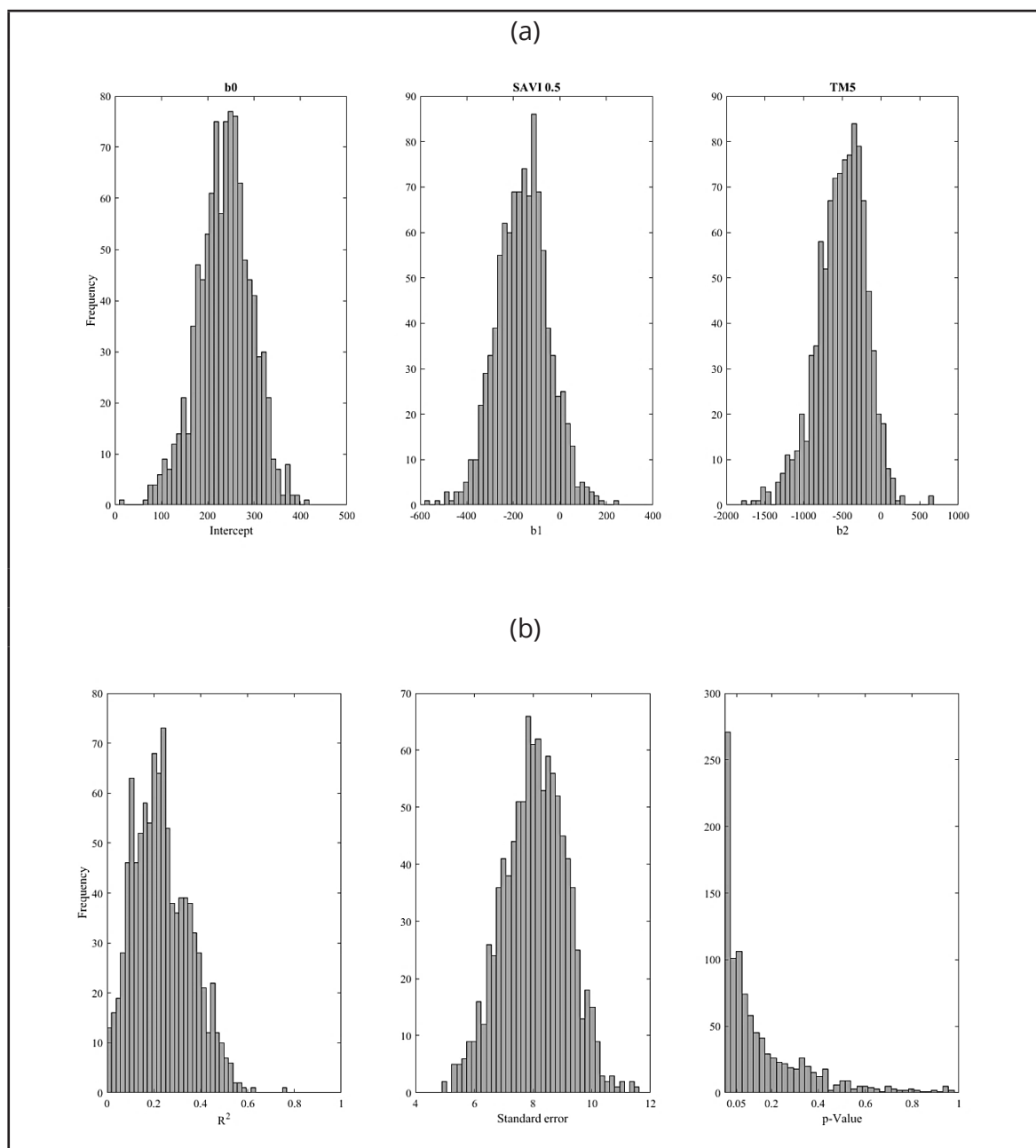
The validation of this model showed a good fit, since the values of the independent variable SAVI 0.5 in none of the simulations had a value equal to zero, which confirms the high significance of this variable in the model (Figure 4a). In addition, considering the statistical criteria (Figure 4b) as the  $R^2$ , the great majority of the values generated in these interactions were concentrated around 0.49, with an estimate of the mean error variance of  $11.69 \text{ m}^3 \text{ ha}^{-1}$ , determined by the large number of occurrences around their mean values and with almost null chance of the model not being significant (values of  $p < 0.05$ ), because only a small number (18) of values generated by the 1,000 permutations obtained p-value higher than 0.05, which represents approximately 2% of the occurrences, and it is possible to state that the model is significant.

However, the model generated for the 34-month *Eucalyptus dunnii* species, the independent variables initially selected in the Pearson correlation matrix did not obtain significant values, resulting in low data adherence to the regression line ( $R^2 = 0.17$ ) and standard error ( $S_{yx} = 8.69 \text{ m}^3 \text{ ha}^{-1}$ ) higher than the 25-month model for *Eucalyptus urograndis*, as evidenced by the low correlation between observed and estimated values of only 41%. Although the variables SAVI 0.5 and TM5 were the best suited ones for the generation of this model, they showed fragility in their fit, since they presented a considerable number of repetitions with values equal to zero (Figure



5a), and  $R^2$  values in their majority ranging from 0.1 to 0.3. Most of their simulations, 644 repetitions, are  $p$ -values greater than the acceptable limit ( $p > 0.05$ ), demonstrating the inefficiency of the model in the generation of VB ( $\text{m}^3 \text{ha}^{-1}$ ) (Figure 5b).

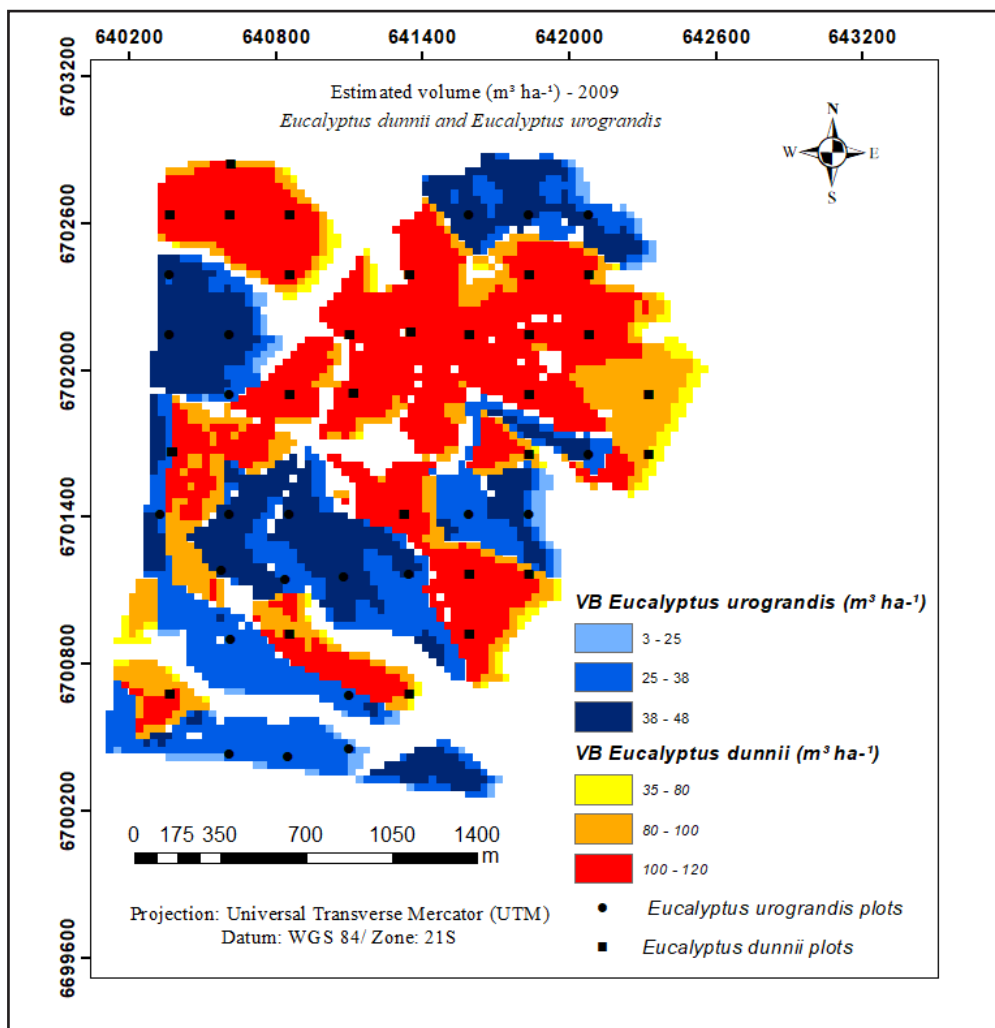
Figure 5 – Prediction model of trade volume with bark in 34-month old *Eucalyptus dunnii* stands. (a) coefficients of the model and; (b) statistical criteria of coefficient of determination ( $R^2$ ), estimation of error variance and  $p$  value, to 95% probability of confidence



Source: Authors (2019)

The significance of the model generated for the *Eucalyptus urograndis* species at initial growth stage shows the distribution surface of the VB values also correspond to the regions where the sample units of this species are distributed (Figure 6). However, the volumetric distribution surface generated for a 34-month-old *Eucalyptus urograndis* species, although the model was not significant, was relevant in the analysis, since it also corresponded with the sample units.

Figure 6 – Distribution map of trade volume with bark (VB -  $m^3 ha^{-1}$ ) of the stands of *Eucalyptus urograndis* and *Eucalyptus dunnii* of 25 and 34 months old, respectively. The squares and points refer to the spatial location of the sample units used in the forest inventory of these species



Source: Authors (2019)

The trend surfaces generated for spatial resolution of 30 m, although they have demonstrated a positive and continuous gradient of volume, in cases where a greater accuracy of details is required, the use of images of high spatial resolution is very useful for providing the canopy structure and closure, to map the distribution space volume more accurately, in addition to better monitoring in the contact regions between different sites (SILVA *et al.*, 2016; MACEDO *et al.*, 2017).

The formation of continuous areas for the models found in this analysis may be due by different conditions of microclimate, soil and site, factors already reported in similar works, in the accuracy of the estimates of the productive capacity of equidistant stands, when using spectral data from optical sensors to model their biophysical parameters (ALBA *et al.*, 2017).

## CONCLUSIONS

In despite of the spatial resolution used (30m), it was efficient in the generation of volumetric modeling of a large area, in this way, serving as a tool suitable for mapping areas quickly and economically compared to conventional forest inventory;

For the three generated models, SAVI 0.5 originated functions with better performance for the representation of VB ( $\text{m}^3 \text{ha}^{-1}$ ) due to the fact that in young stands, 25-month old *Eucalyptus urograndis* and 34-month old *Eucalyptus dunnii*, closing of the tree canopy does not yet occur, demonstrating the greater importance of the soil;

SWIR1 (TM5), although they obtained lower weight in comparison with the SAVI 0.5, of the models for *Eucalyptus urograndis* and *Eucalyptus dunnii* of 50 and 59 months old, respectively and for *Eucalyptus dunnii* of 34 months, was predominant, because this region of the electromagnetic spectrum is related to increased lignin content, demonstrating the importance of the greater interaction with the canopy structure;

It was possible to verify the variation of development within the same plantations of *Eucalyptus* sp. and to obtain statistically significant values of large extensions, in area of regions not inventoried, under the same site conditions, climate and soil, providing valuable information to forest managers.

## ACKNOWLEDGMENTS

Our thanks to the Federal University of Santa Maria – UFSM (Brazil), to Stora Enso Company (Brazil) for allowing the collection and publication of data, and the Coordination of Improvement of Higher Level Personnel - Capes (Brazil), which supported this study by providing the expertise of professors/researchers, infrastructure and funding.

## REFERENCES

- ALBA, E. *et al.* Uso de imagens de média resolução espacial para o monitoramento de dosséis de *Eucalyptus grandis*. **Revista Scientia Agraria**, Curitiba, v. 18, n. 4, p. 1-8, out-dez. 2017.
- ALMEIDA, A. Q. *et al.* Relações empíricas entre características dendrométricas da Caatinga brasileira e dados TM Landsat 5. **Pesquisa Agropecuária Brasileira**, Brasília, v. 49, n. 4, p. 306-315, abr. 2014.
- BERRA, E. F. *et al.* Estimativa do volume total de madeira em espécies de eucalipto a partir de imagens de satélite Landsat. **Ciência Florestal**, Santa Maria, v. 22, n. 4, p. 853-864, out.-dez. 2012.
- BERRA, E. F.; FONTANA, D. C.; KUPLICH, T. M. Tree age as adjustment factor to NDVI. **Árvore**, Viçosa, vol. 41, n. 3, fev. 2017.
- BOLDRINI, I. I. A flora dos campos do Rio Grande do Sul. *In*: PILLAR, V. P.; MÜLLER, S. C.; CASTILHOS, Z. M. S.; JACQUES, A.V. A. (eds.). **Campos Sulinos, conservação e uso sustentável da biodiversidade**. MMA, Brasília, p. 63-77, 2009.
- CANAVESI, V.; PONZONI, F. J.; VALERIANO, M. M. Estimativa de volume de madeira em plantios de *Eucalyptus* spp. utilizando dados hiperespectrais e dados topográficos. **Revista Árvore**, Viçosa, v. 34, n. 3, p. 539-549, jun. 2010.
- CHANDER, G.; MARKHAM, B. L.; BARSÍ, J. A. Revised Landsat-5 thematic mapper radiometric calibration. **Geoscience and Remote Sensing Letters**, Maceió, v. 4, p. 490-494, jul.2007.
- DANIELSSON, J. *et al.* Using a bootstrap method to choose the sample fraction in tail index estimation. **Journal of Multivariate analysis**, Quebec, v. 76, n. 2, p. 226-248, fev. 2001.
- DUBE, T.; MUTANGA, O. Evaluating the utility of the medium-spatial resolution Landsat 8 multispectral sensor in quantifying aboveground biomass in uMgeni catchment, South Africa. **ISPRS Journal of Photogrammetry and Remote Sensing**, Calgary, v. 101, p. 36-46, mar. 2015.
- EFRON, B. **The Jackknife, the Bootstrap, and Other Resampling Plans** CBMS-NSF Regional Conference Series in Applied Mathematics. Society for Industrial & Applied Mathematics, 100p. 1987.

- EFRON, B.; TIBSHIRANI, R. Improvements on cross-validation: the 632+ bootstrap method. **Journal of the American Statistical Association**, Richmond, v. 92, n. 438, p. 548-560, jun. 1997.
- GOEL, N. S. Models of vegetation canopy reflectance and their use in estimation of biophysical parameters from reflectance data. **Remote Sensing Reviews**, Morgantown, v. 4, p. 1-212, dez. 1988.
- GOERGEN, L. C. G. *et al.* Distinção de espécies de eucalipto de diferentes idades por meio de imagens TM/Landsat 5. **Pesquisa Agropecuária Brasileira**, Brasília, v. 51, p. 53-60, jan. 2016.
- GUTMAN, G. *et al.* Assessment of the NASA-USGS Global Land Survey (GLS) datasets. **Remote Sensing of Environment**, Toronto, v. 134, p. 249-265, jul. 2013.
- HUETE, A. R. A soil-adjusted vegetation index (SAVI). **Remote Sensing of Environment**, Toronto, v. 25, p. 295-309, ago. 1988.
- INSTITUTO NACIONAL DE PESQUISAS ESPACIAIS - INPE. Centro de Dados de Sensoriamento Remoto. Catálogo de imagens: satélite Landsat 5. Disponível em: <http://www.dgi.inpe.br/CDSR/>. Acesso em: 15 mar. 2012.
- ITT - VISUAL INFORMATION SOLUTIONS. **Atmospheric correction module: QUAC and FLAASH user's guide**. 2009. 44p.
- KROSS, A. *et al.* Assessment of RapidEye vegetation indices for estimation of leaf area index and biomass in corn and soybean crops. **International Journal of Applied Earth Observation and Geoinformation**, v. 34, p. 235-248, sep. 2015.
- KUINCHTNER, A.; BURIOL, G. A. Clima do Estado do Rio Grande do Sul segundo a classificação climática de Köppen e Thornthwaite. **Disciplinarum Scientia**, Santa Maria, v. 2, p. 171-182, jan-fev. 2001.
- JORDAN, C. F. Derivation of leaf-area index from quality of light on the forest floor. **Ecology**, Davis, v. 50, p. 663-666, jul. 1969.
- LI, S.; QUACKENBUSH, L.J.; IM, J. Airborne Lidar Sampling Strategies to Enhance Forest Aboveground Biomass Estimation from Landsat Imagery. **Remote Sensing**, Flagstaff, v. 11, n. 16, aug. 2019.
- LU, D. *et al.* Relationships between forest stand parameters and Landsat TM spectral responses in the Brazilian Amazon Basin. **Forest Ecology and Management**, Amsterdam, v. 198, n. 1-3, p. 149-167, ago. 2004.
- MACEDO, F. L. *et al.* Estimativa do volume de madeira para *Eucalyptus* sp. com imagens de satélite de alta resolução espacial. **Scientia Forestalis**, Piracicaba, v. 45, n. 114, p. 237-247, jun. 2017.
- NETER, J. *et al.* **Applied Linear Statistical Models**. Chicago: IRWIN, 1996. 1408 p.
- PONZONI, F. J. *et al.* Caracterização espectro temporal de dosséis de *Eucalyptus* spp. mediante dados radiométricos TM/Landsat5. **Cerne**, Lavras, v. 21, p. 267-275, abr-jun. 2015.

REIS, A. A. *et al.* Relationship Between Spectral Data and Dendrometric Variables in *Eucalyptus* sp. stands. **Floresta e Ambiente**, Seropédica, v. 25, n. 2, jun. 2018.

ROUSE, J. W. *et al.* **Monitoring the vernal advancement and retrogradation (green wave effect) of natural vegetation**. Greenbelt: NASA, 1974. 371p.

SANQUETTA, C. R. *et al.* **Inventários florestais: planejamento e execução**. Curitiba: Multi-Graphic Gráfica e Editora, 2014. 406p.

SANTOS, H. G. *et al.* **Sistema brasileiro de classificação de solos**. Brasília: Embrapa, 2013. 353p.

SILVA, C. A. *et al.* A principal component approach for predicting the stem volume in *Eucalyptus* plantations in Brazil using airborne LiDAR data. **Forestry**, Farnham, v. 89, n. 4, p. 422-433, mar. 2016.

SOIL SURVEY STAFF. **Keys to soil taxonomy**. Washington: USDA-NRCS, 2014. 372p.

SOUZA, C. L.; PONZONI, F. J. Relação entre índice de área foliar, estimado através de sensoriamento remoto, e parâmetros dendrométricos em floresta implantada de *Pinus spp.* In: SIMPÓSIO BRASILEIRO DE SENSORIAMENTO REMOTO, 9; 1998, Santos. **Anais...** Santos: INPE/SELPER, 1998, p. 1549-1560.

ZHAO, Q. *et al.* Comparison of machine learning algorithms for forest parameter estimations and application for forest quality assessments. **Forest Ecology and Management**, Arizona, v. 434, p. 224-234, feb. 2019.

WATZLAWICK, L. F.; KIRCHNER, F. F.; SANGUETTA, C. R. Estimativa de biomassa e carbono em floresta com araucária utilizando imagens do satélite IKONOS II. **Ciência Florestal**, Santa Maria, v. 19, p. 169-181, abr.-jun. 2009.

## Authorship Contribution

### 1 – Laura Camila de Godoy Goergen

Forestry Engineer, Dr.

<https://orcid.org/0000-0002-3134-7117> • lauragoergen@yahoo.com.br

Contribution: Conceptualization, Data curation, Formal Analysis, Funding acquisition, Investigation, Methodology, Project administration, Resources, Software, Supervision, Validation, Visualization, Writing – original draft, Writing – review & editing

### 2 – Igor da Silva Narvaes

Forestry Engineer, Dr.

<https://orcid.org/0000-0002-9950-895X> • igor.narvaes@inpe.br

Contribution: Conceptualization, Data curation, Formal Analysis, Investigation, Methodology, Resources, Software, Supervision, Validation, Visualization, Writing – original draft, Writing – review & editing

### 3 – Marcos Adami

Economist, Dr.

<https://orcid.org/0000-0003-4247-4477> • marcos.adami@inpe.br

Contribution: Conceptualization, Formal Analysis, Investigation, Methodology, Software, Supervision, Validation, Visualization, Writing – review & editing

## How to quote this article

Goergen, L. C. G.; Narvaes, I. S.; Adami, M. Estimation of wood volume of *Eucalyptus dunnii* and *Urograndis* of different ages using TM/LANDSAT 5i. *Ciência Florestal*, Santa Maria, v. 31, n. 2, p. 683-704, 2021. DOI 10.5902/1980509834751. Available from: <https://doi.org/10.5902/1980509834751>. Accessed: xx abbreviated-month 2021.